Photon sphere and reentrant phase transition of charged Born-Infeld-AdS black holes

Yu-Meng Xu,[1] Hui-Min Wang,[1] Yu-Xiao Liu,[1] and Shao-Wen Wei[1,2,*]

[1]*Institute of Theoretical Physics & Research Center of Gravitation, Lanzhou University, Lanzhou 730000, People's Republic of China*

[2]*Department of Physics and Astronomy, University of Waterloo, Waterloo, Ontario N2L 3G1, Canada*

(Received 5 July 2019; published 21 November 2019)

Comparing to a charged anti–de Sitter (AdS) black hole in general relativity, a new interesting phase transition—the reentrant phase transition—is observed in a charged Born-Infeld-AdS black hole system. It is worth extending the study of the relationship between the photon sphere and thermodynamic phase transition (especially the reentrant phase transition) to this black hole background. Black hole systems are divided into four cases according to the number of thermodynamic critical points, with different values of the Born-Infeld parameter b, where the black hole systems can have no phase transition, a reentrant phase transition, or a van der Waals-like phase transition. For these different cases, we obtain the corresponding pressure-temperature phase structures and temperature-specific volume diagrams. The tiny differences between these cases are clearly displayed. Then, we calculate the radius r_{ps} and the minimal impact parameter u_{ps} of the photon sphere via the effective potential of the radial motion of photons. r_{ps} and u_{ps} are found to have different behaviors for the different cases. In particular, with the increase of r_{ps} or u_{ps} the temperature exhibits a decrease-increase-decrease-increase behavior for fixed pressure if there is a reentrant phase transition, while for fixed temperature the pressure exhibits an increase-decrease-increase-decrease behavior instead. These behaviors are quite different from that of the van der Waals-like phase transition. Near the critical point, the behavior of r_{ps} and u_{ps} for the black hole phase transitions confirms a universal critical exponent of $\frac{1}{2}$. We also find that the temperature and pressure corresponding to the extremal points of r_{ps} and u_{ps} are highly consistent with the thermodynamic metastable curve for black hole systems with different values of b. Furthermore, we also extend the corresponding study to higher-dimensional black holes cases. The results show that the photon sphere behaves quite differently for the van der Waals-like and reentrant phase transitions, and both phase transitions can be identified via the photon sphere.

DOI: 10.1103/PhysRevD.100.104044

I. INTRODUCTION

Since the establishment of the four laws of black hole thermodynamics [1,2] phase transitions have been an attractive and valuable subject in gravitational physics. Of particular interest are phase transitions in anti–de Sitter (AdS) space, where a negative cosmological constant Λ was interpreted as the pressure P [3–5],

$$P = -\frac{\Lambda}{8\pi}. \tag{1}$$

The corresponding conjugate quantity is the thermodynamic volume of the black hole system. After including this pressure and volume term, the first law of black hole thermodynamics coincides exactly with that of an ordinary thermodynamic system. The inconsistency of the first law and the Smarr formula for a rotating AdS black hole has also been established. Moreover, the small-large black hole phase transition was identified with the liquid-gas phase transition of a van der Waals (VdW) fluid [6]. More interesting phase transitions have also been found [7–23]. In particular, near the critical point black hole systems were found to possess the same critical phenomena as a VdW fluid. This to some extent implies that these thermodynamic systems may share a similar microstructure, and the issue was further investigated in Ref. [23].

Interestingly, information about a black hole's phase transition is also expected to be encoded in or revealed by its dynamic and gravitational properties. Therefore, studying the relationship between them can bridge studies of these two subjects.

Quasinormal modes (QNMs) are dynamical perturbations, and they can provide us with significant observational signatures to test the natural properties of these black

*weishw@lzu.edu.cn

holes. The subject of probing the black hole phase transition using QNMs was numerically investigated in Ref. [24]. For a charged Reissner-Nordström black hole, it was found that when the black hole charge exceeds the Davies point, the QNM frequency ω takes on a spiral-like shape in the complex ω plane. The Davies point is related to the divergence point of the heat capacity, so this point actually measures a black hole phase transition between an unstable phase and a stable phase. Some further studies on this issue can be found in Refs. [25–29].

For the VdW-like phase transition of a charged AdS black hole, the result given in Ref. [30] suggests that the QNMs have different slopes along the small and large black hole phases. Thus, this signature can be used to test the first-order small-large black hole phase transition. However, it was argued that this method was only accurate for low pressure or temperature, and when the black hole system approaches its critical case the QNMs become more complicated, and thus one must be very careful with these cases. This method was also extended to other AdS black hole systems [31–40]. All of these results imply that the VdW-like phase transition can be identified by the slope of the QNMs. Another interesting point is whether the reentrant phase transition can be identified from the behavior of QNMs and how to distinguish it from the VdW-like phase transition, since the isothermal and isobaric lines are more complicated. Thus, we believe that besides the slope of the QNMs, more subtle information about the QNMs should be included. Therefore, this issue deserves further study, and we will not discuss it here.

On the other hand, the geodesics of a test particle around a black hole is closely related to strong gravitational effects, such as lensing and shadows. Studying the relationship between geodesics and black hole thermodynamics will give us a novel way to test phase transitions by using these observables. This will also open a new window to study black hole thermodynamics using astronomical observations. Keeping this in mind, we studied the behavior of the photon sphere of a charged AdS black hole when the VdW-like phase transition occurs [41]. Two key quantities—the radius and the minimal impact parameter of the photon sphere—were found to behave quite differently depending on whether there is a VdW-like phase transition. These two quantities also experience sudden changes when the phase transition takes place. These changes decrease with the temperature and tend to vanish at the critical point. Further calculation also showed that these changes in the radius and minimal impact parameter have a universal critical exponent of $\frac{1}{2}$, which implies that these changes can serve as an order parameter to describe the small-large black hole phase transition. Subsequently, we extended our study to rotating Kerr-AdS black holes [42]. Even when a black hole is rotating, our results showed that a similar relationship between the photon ring and the phase transition also holds. Moreover, it was found that the temperature and pressure corresponding to the extremal points of the radius and minimal impact parameter are highly consistent with the thermodynamic metastable curve for Kerr-AdS black holes. This study was also generalized to other black hole backgrounds [43–46]. For example, the authors of Ref. [43] studied the relation between the thermodynamic phase transition and the circular orbits of charged test particles. Photon orbits and thermodynamic phase transitions were examined in Gauss-Bonnet AdS black holes [44], massive black holes [43], and even in a general spherically symmetric spacetime [46]. In addition, the presence of a photon orbit also reveals a York-Hawking-Page-type phase transition of spacetimes [47–49].

Apart from the VdW-like phase transition, there are some other interesting phase transitions, such as the reentrant phase transition. Therefore, it is of great interest to examine the relationship between the photon sphere and the reentrant phase transition. As we know, charged Born-Infeld (BI)-AdS black holes demonstrate a typical reentrant phase transition [7,17]. Therefore, it is valuable to extend our previous study and examine the relationship for BI-AdS black holes. These will reveal the novel behavior of the photon sphere during the reentrant phase transition.

This work is organized as follows. In Sec. II we give a brief review of the thermodynamics of BI-AdS black holes. Then, we study four different black hole cases with different values of the BI parameter b. The corresponding reentrant phase structure and VdW-like phase structure are displayed in P-T and T-v diagrams, respectively. We analyze the thermodynamic properties of each case. In Sec. III we determine the radius and minimal impact parameter of the photon sphere by using the effective potential of radial motion. Then, for each different case we study the behavior of the pressure and temperature as a function of $r_{\rm ps}$ or $u_{\rm ps}$, respectively. When the reentrant phase transition takes place, the temperature and pressure behave quite differently from that of the VdW-like phase transition. Furthermore, near the critical point we confirm that the changes $\Delta r_{\rm ps}$ and $\Delta u_{\rm ps}$ have a universal critical exponent of $\frac{1}{2}$, which is the same as that of the VdW-like phase transition for charged-AdS or rotating Kerr-AdS black holes. The temperature and pressure corresponding to the extremal points of $r_{\rm ps}$ and $u_{\rm ps}$ are also found to be highly consistent with the thermodynamic metastable curve for BI-AdS black hole systems even when there is no reentrant or VdW-like phase transition. In Sec. IV we study the relation between the photon sphere and the small-large black hole phase transition. The critical exponents of $\Delta r_{\rm ps}$ and $\Delta u_{\rm ps}$ are also calculated. Finally, our conclusions and discussions are presented in Sec. V.

II. THERMODYNAMICS AND PHASE STRUCTURE

For a four-dimensional charged BI-AdS black hole, it was found that due to the values of the BI parameter there may exist a VdW-like phase transition, i.e., the reentrant phase transition [7]. However, a VdW-like phase transition only exists for the higher-dimensional black hole cases [8]. When studying black hole phase transitions it is interesting to examine the phase diagram, using which one could easily identify the type of phase transition that occurs in different parameter ranges. In this section, we briefly review the phase transition. In Refs. [7,8] the phase diagram was given as a P-T diagram. However, the coexistence region is only one curve in that diagram. In order to display the coexistence region we investigate the phase diagram using a T-v diagram, and study the difference between the VdW-like and reentrant phase transitions.

The action describing a BI-AdS black hole is

$$I_{\mathrm{EM}} = -\frac{1}{16\pi}\int_M \sqrt{-g}\left(R + \mathcal{L}_{\mathrm{BI}} + \frac{6}{l^2}\right), \tag{2}$$

where the BI term is

$$\mathcal{L}_{\mathrm{BI}} = 4b^2\left(1 - \sqrt{1 + \frac{1}{2b^2}F^{\mu\nu}F_{\mu\nu}}\right). \tag{3}$$

Here the AdS radius l is related to the pressure as $P = \frac{3}{8\pi l^2}$. The BI parameter b denotes the maximal electromagnetic-field strength, and is related to the string tension. By solving the corresponding Einstein equations one can obtain the following black hole solution:

$$ds^2 = -f(r)dt^2 + \frac{dr^2}{f(r)} + r^2(d\theta^2 + \sin^2\theta d\phi^2), \tag{4}$$

$$F = \frac{Q}{\sqrt{r^4 + Q^2/b^2}}dt \wedge dr. \tag{5}$$

The metric function is given by

$$\begin{aligned} f(r) &= 1 - \frac{2M}{r} + \frac{r^2}{l^2} + \frac{2b^2}{r}\int_r^\infty \left(\sqrt{r^4 + \frac{Q^2}{b^2}} - r^2\right)dr \\ &= 1 - \frac{2M}{r} + \frac{r^2}{l^2} + \frac{2b^2r^2}{3}\left(1 - \sqrt{1 + \frac{Q^2}{b^2r^4}}\right) \\ &\quad + \frac{4Q^2}{3r^2}{}_2F_1\left(\frac{1}{4},\frac{1}{2};\frac{5}{4};-\frac{Q^2}{b^2r^4}\right). \end{aligned} \tag{6}$$

Here ${}_2F_1$ is the hypergeometric function. The parameters M and Q are the black hole mass and charge, respectively. By solving $f(r_+) = 0$ we can express the black hole mass as

$$\begin{aligned} M &= \frac{r_+}{2} + \frac{r_+^3}{2l^2} + \frac{b^2r_+^3}{3}\left(1 - \sqrt{1 + \frac{Q^2}{b^2r_+^4}}\right) \\ &\quad + \frac{2Q^2}{3r_+}{}_2F_1\left(\frac{1}{4},\frac{1}{2};\frac{5}{4};-\frac{Q^2}{b^2r_+^4}\right), \end{aligned} \tag{7}$$

where r_+ is the radius of the black hole horizon. Using the "Euclidean trick," one can obtain the black hole temperature as

$$T = \frac{1}{4\pi r_+}\left(1 + \frac{3r_+^2}{l^2} + 2b^2r_+^2\left(1 - \sqrt{1 + \frac{Q^2}{b^2r_+^4}}\right)\right). \tag{8}$$

According to the Bekenstein-Hawking area-entropy relation, the black hole entropy can be calculated as

$$S = \frac{A}{4} = \pi r_+^2, \tag{9}$$

where $A = 4\pi r_+^2$ is the area of the black hole horizon. The electric potential and the electric polarization measured at infinity with respect to the horizon are

$$\Phi = \frac{Q}{r_+}{}_2F_1\left(\frac{1}{4},\frac{1}{2};\frac{5}{4};-\frac{Q^2}{b^2r_+^4}\right), \tag{10}$$

$$B = \frac{2}{3}br_+^3\left(1 - \sqrt{1 + \frac{Q^2}{b^2r_+^4}} + \frac{Q^2}{3br_+}\right){}_2F_1\left(\frac{1}{4},\frac{1}{2};\frac{5}{4};-\frac{Q^2}{b^2r_+^4}\right). \tag{11}$$

The Gibbs free energy is

$$\begin{aligned} G(T,P) &= \frac{1}{4}\left(r_+ - \frac{8\pi}{3}Pr_+^3 - \frac{2b^2r_+^3}{3}\left(1 - \sqrt{1 + \frac{Q^2}{b^2r_+^4}}\right)\right. \\ &\quad \left. + \frac{8Q^2}{3r_+}{}_2F_1\left(\frac{1}{4},\frac{1}{2};\frac{5}{4};-\frac{Q^2}{b^2r_+^4}\right)\right). \end{aligned} \tag{12}$$

Employing these thermodynamic quantities, one can check that the following first law and Smarr formula hold:

$$dM = TdS + VdP + \Phi dQ + Bdb, \tag{13}$$

$$M = 2(TS - VP) + \Phi Q - Bb, \tag{14}$$

with the thermodynamic volume $V = \frac{4\pi r_+^3}{3}$. Identifying the specific volume $v = 2r_+$, we can obtain the state equation from Eq. (8),

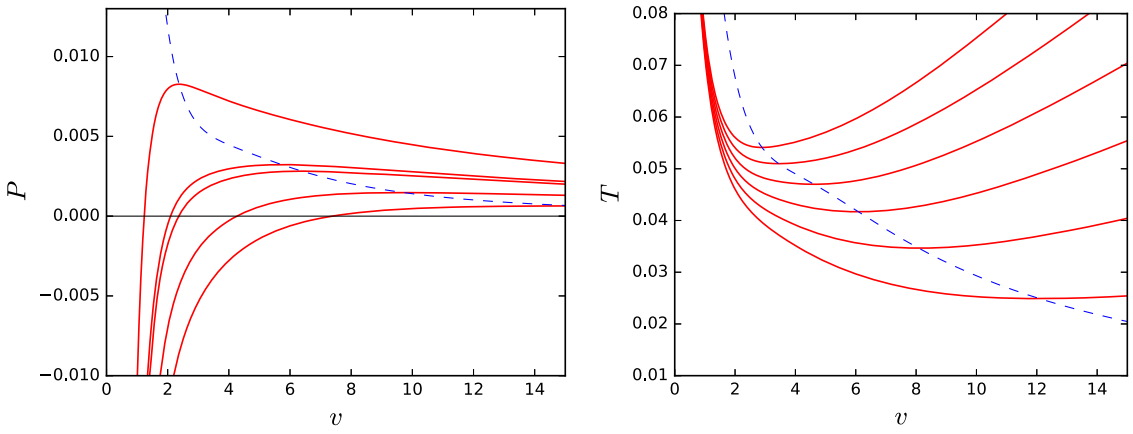

(a) Isothermal curves (b) Isobaric curves

FIG. 1. Case I: Isothermal and isobaric curves of BI-AdS black holes for $b = 0.3 < b_0$. (a) Isothermal curves with temperature $T = 0.02, 0.03, 0.04, 0.043$, and 0.06 from bottom to top. (b) Isobaric curves with pressure $P = 0.001, 0.002, 0.003, 0.004, 0.005$, and 0.006 from bottom to top. The dashed curves describe the extremal points of the isothermal and isobaric curves.

$$P = \frac{T}{v} - \frac{1}{2\pi v^2} - \frac{b^2}{4\pi}\left(1 - \sqrt{1 + \frac{16Q^2}{b^2 v^4}}\right). \tag{15}$$

This state equation is found to have a VdW-like phase transition or a reentrant phase transition depending on the value of the BI parameter b. The corresponding critical points can be obtained by solving

$$(\partial_v P)_T = 0, \qquad (\partial_v^2 P)_T = 0, \tag{16}$$

and they are given by [7]

$$\begin{aligned} T_c &= \frac{1 - 8xQ^2}{\pi v_c}, \\ P_c &= \frac{1 - 16xQ^2}{2\pi v_c^2} - \frac{b^2}{4\pi}\left(1 - \frac{1}{v_c^2 x}\right), \\ v_c &= \left(\frac{1}{x_k^2} - \frac{16Q^2}{b^2}\right)^{\frac{1}{4}}, \end{aligned} \tag{17}$$

with

$$x_k = 2\sqrt{-\frac{p}{3}}\cos\left(\frac{1}{3}\arccos\left(\frac{3q}{2p}\sqrt{\frac{-3}{p}}\right) - \frac{2\pi k}{3}\right), \quad k = 0, 1, 2, \tag{18}$$

$$p = -\frac{3b^2}{32Q^2}, \qquad q = \frac{b^2}{256Q^4}. \tag{19}$$

For x_2, the value of the corresponding critical point is always a complex number. Therefore, we have two critical points at most. Following Ref. [7], we can divide the parameter range of b into four cases:

Case I: $b < b_0$. This case is similar to a Schwarzschild-AdS black hole. It consists of a stable large black hole phase and an unstable small black hole phase. However, there do not exist the VdW-like phase transition and the critical point.

Case II: $b_0 < b < b_1$. The case has two positive critical points c_0 and c_1. However, c_0 has a higher Gibbs free energy, and thus it is a globally unstable point. For this case, there exists a first-order phase transition and a "zeroth"-order phase transition, which is a typical reentrant phase transition.

Case III: $b_1 < b < b_2$. This case is similar to case II, where a reentrant phase transition exists. The only difference is that the critical point c_0 has a negative pressure.

Case IV: $b_2 < b$. Only one critical point c_1 exists for this case. The phase transition for this case is the VdW-type phase transition.

The values of the parameters b_i are given by

$$b_0 = \frac{1}{\sqrt{8}Q} \approx \frac{0.3536}{Q}, \qquad b_1 = \frac{\sqrt{3 + 2\sqrt{3}}}{6Q} \approx \frac{0.4237}{Q}, \qquad b_2 = \frac{1}{2Q} = \frac{0.5}{Q}. \tag{20}$$

In the following we take $Q = 1$ for simplicity. We plot the isothermal and isobaric curves of these four cases in Figs. 1–4. All of the different properties can be found. In particular, the blue dashed lines are for metastable curves, which are defined by

$$(\partial_v P)_T = 0, \quad \text{or} \quad (\partial_v T)_P = 0. \tag{21}$$

From these figures, one finds that the metastable curves have no extremal point for $b < b_0$, two extremal points for

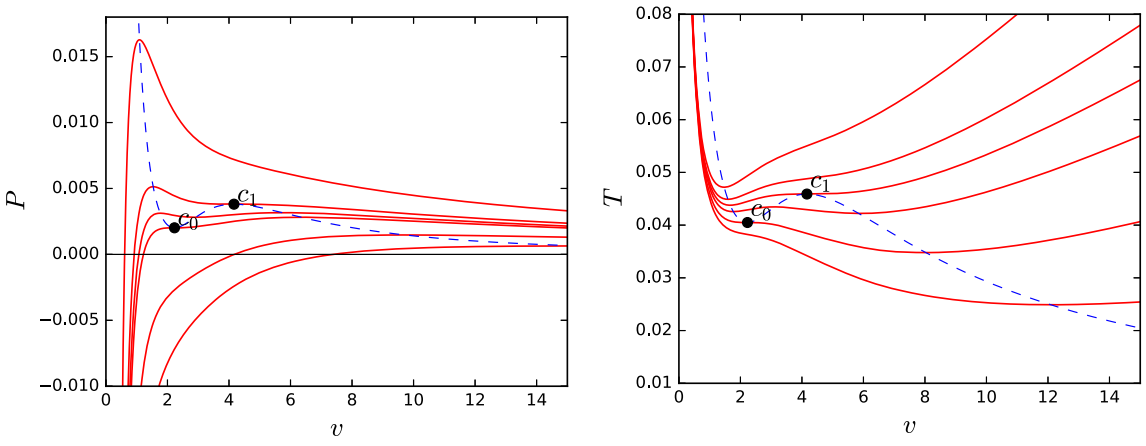

(a) Isothermal curves (b) Isobaric curves

FIG. 2. Case II: Isothermal and isobaric curves of BI-AdS black holes for $b = 0.4 \in (b_0, b_1)$. (a) Isothermal curves with temperature $T = 0.02$, 0.03, 0.040492 (T_{c0}), 0.043, 0.045890 (T_{c1}), and 0.06 from bottom to top. (b) Isobaric curves with pressure $P = 0.001$, 0.002016 (P_{c0}), 0.003, 0.003807 (P_{c1}), 0.0045, and 0.006 from bottom to top. As opposed to Fig. 1, for certain values of the pressure and temperature the number of extremal points can be more than one. These two critical points are marked as black dots, which both have positive pressure and temperature. However, the critical point located at (T_{c0}, P_{c0}) has a higher Gibbs free energy, so it is not a global stable point.

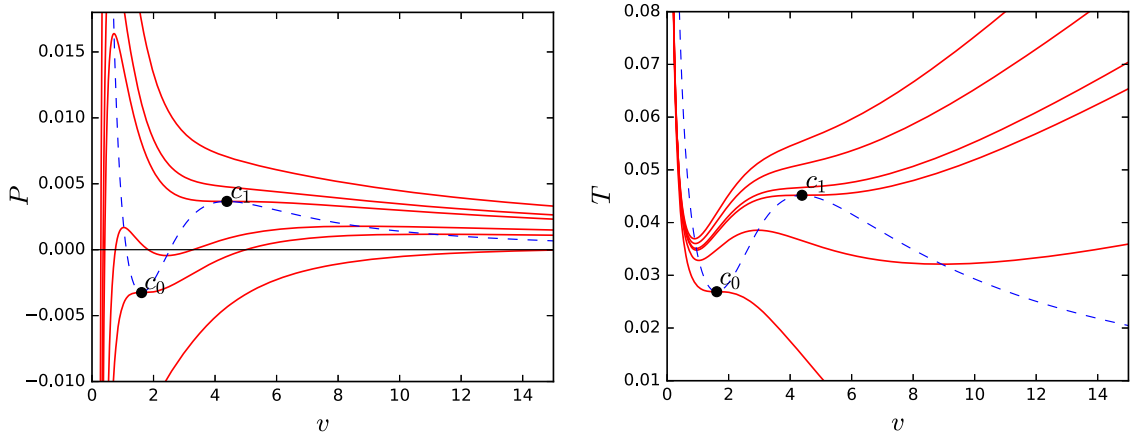

(a) Isothermal curves (b) Isobaric curves

FIG. 3. Case III: Isothermal and isobaric curves of BI-AdS black holes for $b = 0.45 \in (b_1, b_2)$. (a) Isothermal curves with temperature $T = 0.01$, 0.026885 (T_{c0}), 0.03, 0.045170 (T_{c1}), 0.05, and 0.06 from bottom to top. (b) Isobaric curves with pressure $P = -0.003253$ (P_{c0}), 0.001,0.002, 0.003, 0.003664 (P_{c1}), and 0.006 from bottom to top. There are two critical points. The second one has a negative pressure and positive temperature, and thus it is unphysical.

$b \in (b_0, b_2)$, and one point for $b > b_2$. Actually, the extremal points are exactly the critical point of the thermodynamic phase transition. In summary, we find a reentrant phase transition for $b \in (b_0, b_2)$ and a VdW-like phase transition for $b > b_2$.

The new type of phase transition—the reentrant phase transition—can be understood by studying the Gibbs free energy. We show the VdW and reentrant phase transition in Fig. 5(a) and 5(b), respectively. In Fig. 5(a) we can see a typical swallow-tail behavior, which indicates a small-large black hole phase transition at $T_0 = 0.033067$. Actually, as the temperature increases the system prefers the small black hole phase as it has a low Gibbs free energy. Until the temperature T_0 is reached the large black hole will have a lower Gibbs free energy, so the system will prefer the large black hole phase. Thus, at T_0 the small-large black hole phase transition takes place, which is similar to the liquid-gas phase transition of a VdW fluid. The case of the reentrant phase transition is more complicated. Taking $P = 0.001685$ and $b = 0.45$, we show the behavior of the Gibbs free energy in Fig. 5(b). When $T < T_1 = 0.031992$, there is no black hole phase. With the increase of the temperature

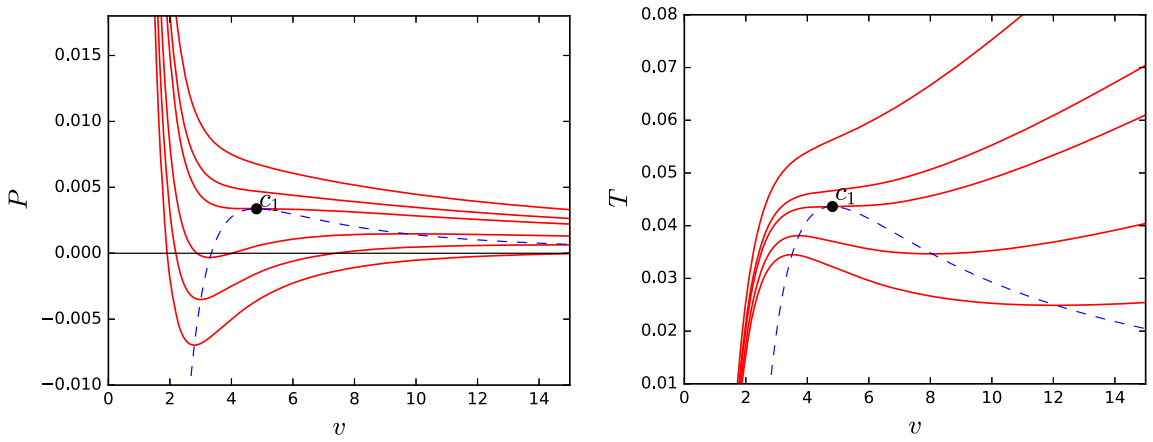

(a) Isothermal curves (b) Isobaric curves

FIG. 4. Case IV: Isothermal and isobaric curves of BI-AdS black holes for $b = 1 > b_2$. (a) Isothermal curves with pressure $P = 0.01$, 0.02, 0.03, 0.043620 (T_{c1}), 0.05, and 0.06 from bottom to top. (b) Isobaric curves with temperature $T = 0.001$, 0.002, 0.003372 (P_{c1}), 0.004, and 0.006 from bottom to top. For this case, only one critical point exists, and we observe the typical VdW-like phase transition.

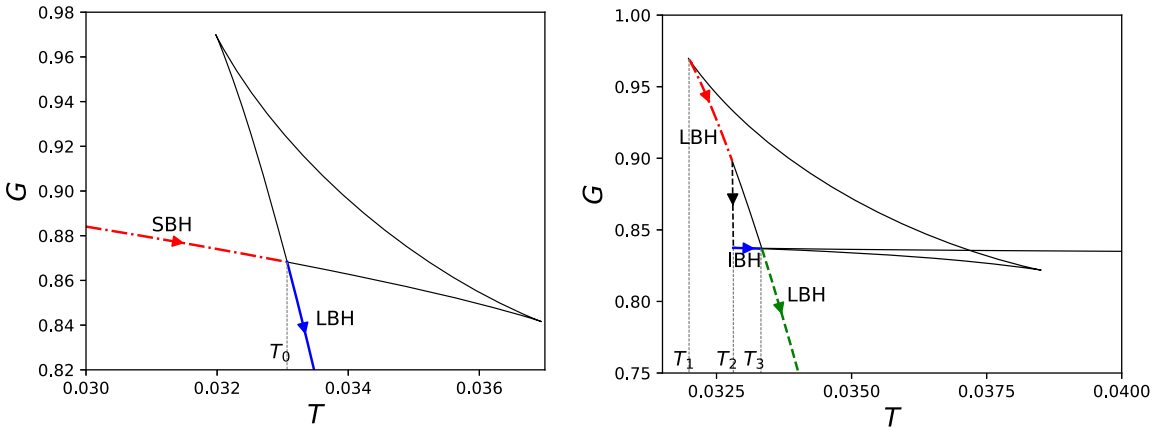

(a) (b)

FIG. 5. The behavior of the Gibbs free energy. (a) A VdW-like phase transition with $P = 0.001685$ and $b = 1$. (b) A reentrant phase transition with $P = 0.001685$ and $b = 0.45$. The temperatures are $T_0 = 0.033067$, $T_1 = 0.031992$, $T_2 = 0.032812$, and $T_3 = 0.033322$.

and according to the fact that a thermodynamic system always prefers a low Gibbs free energy phase, the spacetime will have a large black hole phase when $T_1 < T < T_2$. At T_2, a phase transition occurs between a large black hole and an intermediate black hole, which is of "zeroth" order. As the temperature increases further, another first-order phase transition between an intermediate black hole and a large black hole takes place at T_3. This behavior of the Gibbs free energy admits a typical reentrant phase transition.

Next, we study the phase structure for BI-AdS black holes. The results are shown in Figs. 6–8 for $b > b_0$. For $b < b_0$, only a stable large black hole phase exists, and thus no phase transition occurs for constant charge.

As mentioned above, for $b \in (b_0, b_1)$ there exists a reentrant phase transition, which is different from the VdW-like phase transition. Taking $b = 0.4$ as an example, we plot the phase structure in Fig. 6. In Fig. 6(a) we show the phase structure in the P-T diagram, which is a typical reentrant phase diagram. The blue solid line denotes the coexistence curve of the intermediate and large black holes, which is a first-order phase transition. The short red dashed curve describes the "zeroth"-order phase transition between the large and intermediate black hole. It is worth noting that this curve is not the coexistence curve of the large and intermediate black holes. It belongs to the intermediate black hole phase because at that point the intermediate black hole has a lower Gibbs free energy than the large black hole. The dot-dashed curves show the extremal points of the isothermal and isobaric curves of BI-AdS black holes. The intersection points of these extremal-point curves (marked with two black dots) are the two

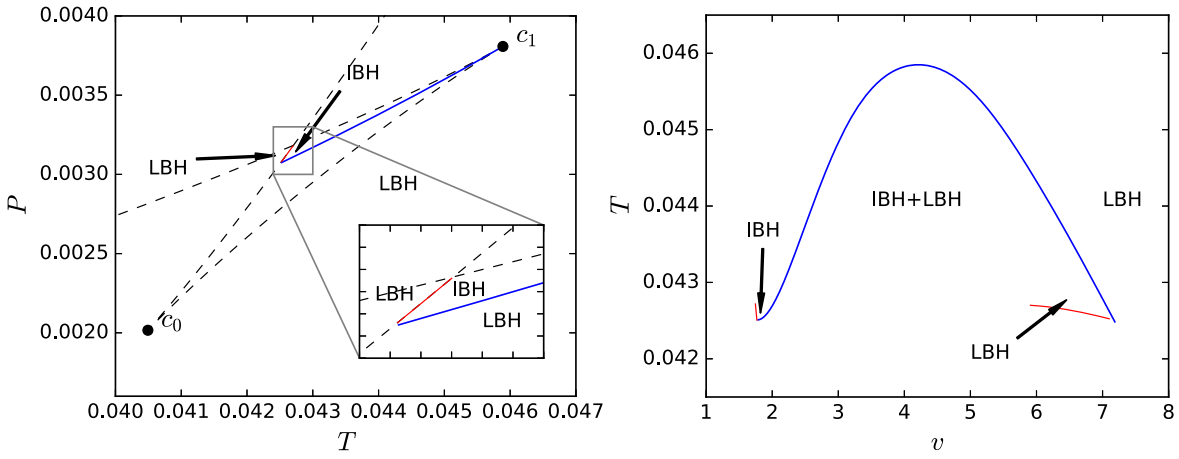

(a) P-T phase diagram (b) T-v phase diagram

FIG. 6. Phase structures of BI-AdS black holes for $b = 0.4 \in (b_0, b_1)$. (a) P-T phase diagram. (b) T-v phase diagram. The blue solid curves are the coexistence curves. The thin red solid curves are the "zeroth"-order phase transition curves. The dot-dashed curves are the extremal-point curves of the isothermal and isobaric curves of BI-AdS black holes. Black dots denote the critical points.

critical points. It is clear that these critical points have positive temperature. On the other hand, the upper left corners bounded by these two extremal point curves are the regions without any black holes.

In order to clearly show the coexistence region of the intermediate and large black holes, we plot the phase structure in the T-v diagram in Fig. 6(b). Below the blue solid curve is the region of coexistence of intermediate and large black holes. The intermediate black hole region is on the left, and the large black hole region is on the right. Since small black holes are thermodynamically unstable, we do not show them. Of particular interest is that there is also a region for the large black hole, which is located in the lower right corner of the coexistence region. Although it overlaps with the coexistence region, it is a large black hole region. The reason for this is that we have a degeneracy in the T-v diagram. So if the phase structure is displayed in another diagram, such a degeneracy could be eliminated.

For the BI parameter $b \in (b_1, b_2)$, there is also a reentrant phase transition. We take $b = 0.45$, and plot the phase structures in the P-T and T-v diagrams in Fig. 7. These phase diagrams are quite similar to the case $b = 0.4$. The tiny difference is that one of the critical points has negative pressure [see Fig. 7(a)], where the critical points are shown as black dots.

When $b > b_2$ the reentrant phase transition disappears, and only the standard VdW-like phase transition is left. The phase diagram is shown in Fig. 8 for $b = 1$.

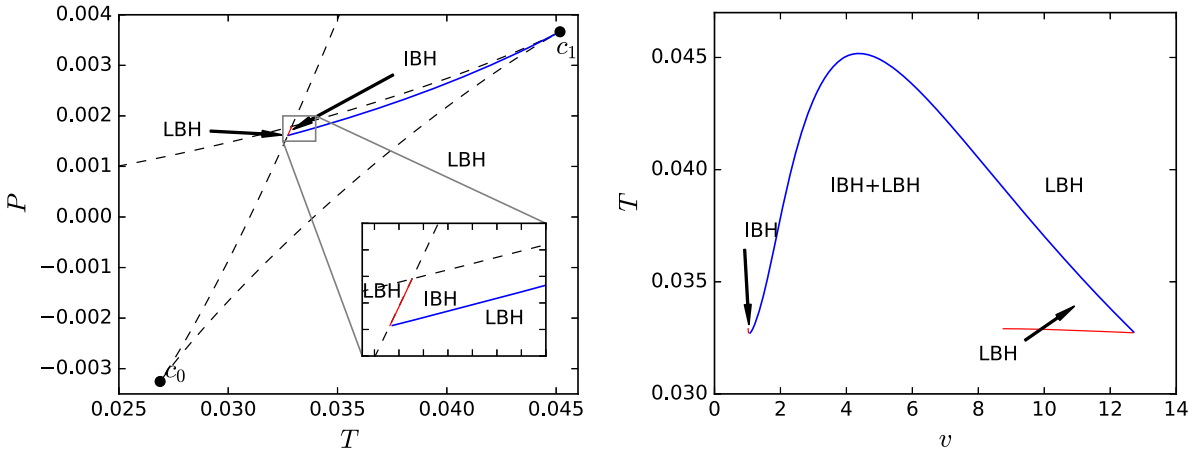

(a) P-T phase diagram (b) T-v phase diagram

FIG. 7. Phase structures of BI-AdS black holes for $b = 0.45 \in (b_1, b_2)$. (a) P-T phase diagram. (b) T-v phase diagram. The blue solid curves are the coexistence curves. The thin red solid curves are the "zeroth"-order phase transition curves. The dot-dashed curves are the extremal point curves of the isothermal and isobaric curves of BI-AdS black holes. Black dots denote the critical points.

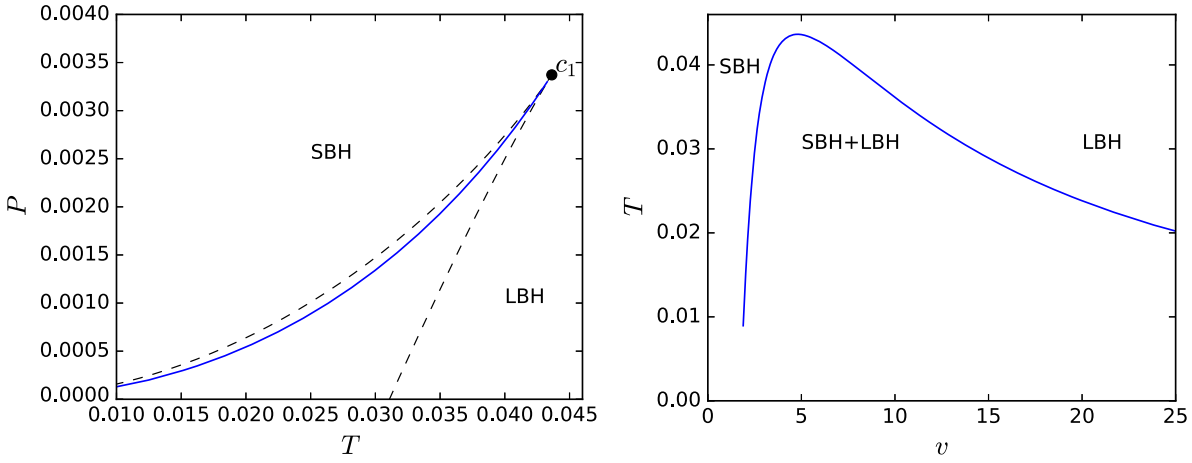

(a) P-T diagram (b) T-v diagram

FIG. 8. Phase structures of BI-AdS black holes for $b = 1 > b_2$ in the P-V and T-v diagrams.

The coexistence curves are plotted as the blue solid curves, and the extremal-point curves are shown by the dot-dashed curves. The P-T phase diagram is shown in Fig. 8(a). Above the coexistence curve is the small black hole phase region, and below it is the large one. The T-v phase diagram is shown in Fig. 8(b). The coexistence phase of small and large black holes is below the coexistence curve. The small and large black hole phases are located to the left and right of the coexistence curve, respectively.

In summary, a VdW-like or reentrant phase transition can be found in different parameter regions of b. The T-v phase diagrams are quite different for these two types of phase transitions.

III. NULL GEODESICS AND PHASE TRANSITIONS

In this section, we study the null geodesics—in particular, the photon sphere—of BI-AdS black holes. Then, we examine the relation between the parameter properties of the photon sphere and the thermodynamic phase transition.

A. Null geodesics and the photon sphere

We consider the motion of a free photon orbiting around a BI-AdS black hole. Since the black hole is spherically symmetric, we fix $\theta = \frac{\pi}{2}$ without loss of generality. Then the Lagrangian of a free photon in the background of a BI-AdS black hole reads

$$\mathcal{L} = \frac{1}{2} g_{\mu\nu} \dot{x}^\mu \dot{x}^\nu = \frac{1}{2}(-f(r)\dot{t}^2 + \dot{r}^2/f(r) + r^2\dot{\phi}^2). \quad (22)$$

A dot denotes ordinary differentiation with respect to an affine parameter. Using the Lagrangian (22), the generalized momentum can be calculated as

$$p_\mu = \frac{\partial \mathcal{L}}{\partial \dot{x}^\mu} = g_{\mu\nu}\dot{x}^\nu. \quad (23)$$

This spacetime has two Killing vectors ∂_t and ∂_ϕ. Thus, for each geodesic there are two constants: the energy E and the orbital angular momentum L of the photon. Considering them, the generalized momenta can be expressed as

$$p_t = -f(r)\dot{t} = -E, \quad p_r = \frac{\dot{r}}{f(r)}, \quad p_\phi = r^2\dot{\phi} = L. \quad (24)$$

A photon is required to satisfy $g_{\mu\nu}\dot{x}^\mu \dot{x}^\nu = 0$. Thus, the radial r motion is

$$\dot{r}^2 + V_{\text{eff}} = 0, \quad (25)$$

where the effective potential is given by

$$V_{\text{eff}} = \frac{L^2}{r^2} f(r) - E^2. \quad (26)$$

Using the effective potential (26), the unstable photon sphere can be obtained by solving

$$V_{\text{eff}} = 0, \quad \partial_r V_{\text{eff}} = 0, \quad \partial_{r,r} V_{\text{eff}} < 0. \quad (27)$$

The first equation gives the minimum impact parameter

$$u_{\text{ps}} = \left.\frac{L}{E}\right|_{r_{\text{ps}}} = \left.\frac{r}{\sqrt{f(r)}}\right|_{r_{\text{ps}}}. \quad (28)$$

Then, by using the second equation one can find that the radius of the photon sphere is determined by the following equation:

$$2f(r_{\text{ps}}) - r_{\text{ps}}\partial_r f(r_{\text{ps}}) = 0. \quad (29)$$

Plugging the metric function (6) into this equation, we obtain

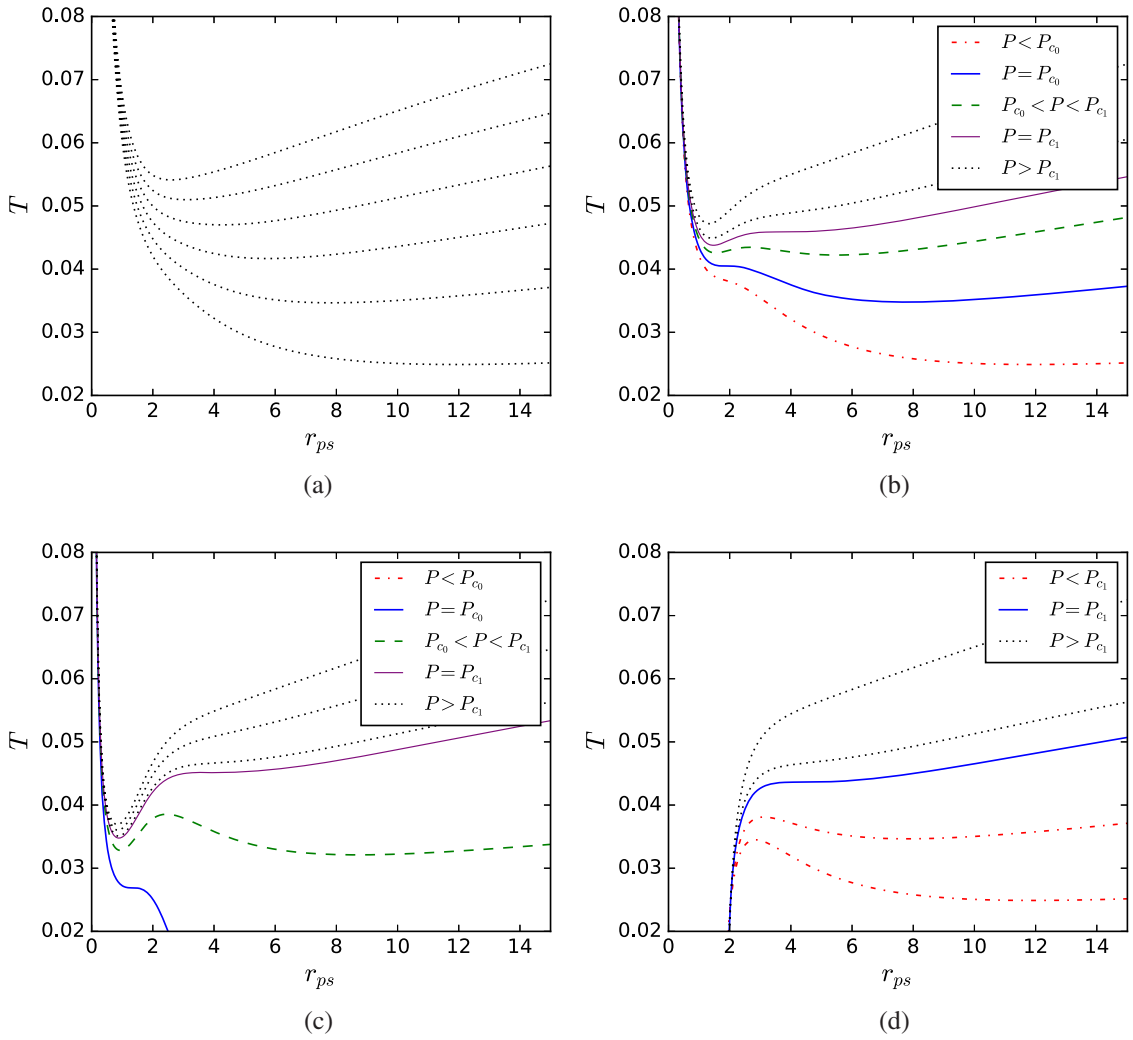

FIG. 9. The temperature T as a function of the radius $r_{\rm ps}$ of the photon sphere for different values of the BI parameter b with fixed pressure P. (a) $b = 0.3 < b_0$ with $P = 0.001$, 0.002, 0.003, 0.004, 0.005, and 0.006 from bottom to top. (b) $b = 0.4 \in (b_0, b_1)$ with $P = 0.001, 0.002016$ ($P_{\rm c0}$), 0.003, 0.003807 ($P_{\rm c1}$), 0.0045, and 0.006 from bottom to top. (c) $b = 0.45 \in (b_1, b_2)$ with $P = -0.003253$ ($P_{\rm c0}$), 0.001,0.002, 0.003, 0.003664 ($P_{\rm c1}$), and 0.006 from bottom to top. (d) $b = 1 > b_2$ with $P = 0.01$, 0.02, 0.03, 0.043620 ($T_{\rm c1}$), 0.05, and 0.06 from bottom to top.

$$r_{\rm ps}^2 - 3Mr_{\rm ps} + 2Q^2 {}_2F_1\left(\frac{1}{4},\frac{1}{2};\frac{5}{4};-\frac{Q^2}{b^2 r_{\rm ps}^4}\right) = 0. \quad (30)$$

For $b = 0$, one gets $r_{\rm ps} = \frac{1}{2}(3M + \sqrt{9M^2 - 8Q^2})$, which is the radius of the photon sphere for a Reissner-Nordström AdS black hole. However, when $b \neq 0$, there is no analytic result.

B. Phase transitions and the photon sphere

For given b and Q, we can solve the radius of the photon sphere using Eq. (30). By substituting the radius into Eq. (28) we can obtain the minimum impact parameter. In order to examine the relation between the photon sphere and the phase transition we study the behavior of the radius and minimum impact parameter along the isothermal and isobaric curves of BI-AdS black holes.

In Fig. 9 we show the temperature T as a function of the radius $r_{\rm ps}$ of the photon sphere at constant pressures for different values of the parameter b. In Fig. 9(a) the pressure $P = 0.001$, 0.002, 0.003, 0.004, 0.005, and 0.006 (from bottom to top), and the BI parameter $b = 0.3 < b_0$, which corresponds to the first case. For this case, T first decreases and then increases with respect to $r_{\rm ps}$. As shown in Refs. [41,42], this behavior of T reveals that no VdW-like phase transition occurs. In Figs. 9(b) and 9(c) we show the results for $b = 0.4$ and 0.45, which are related to cases II and III given above. For these two cases, BI-AdS black holes exhibit a reentrant phase transition. From these

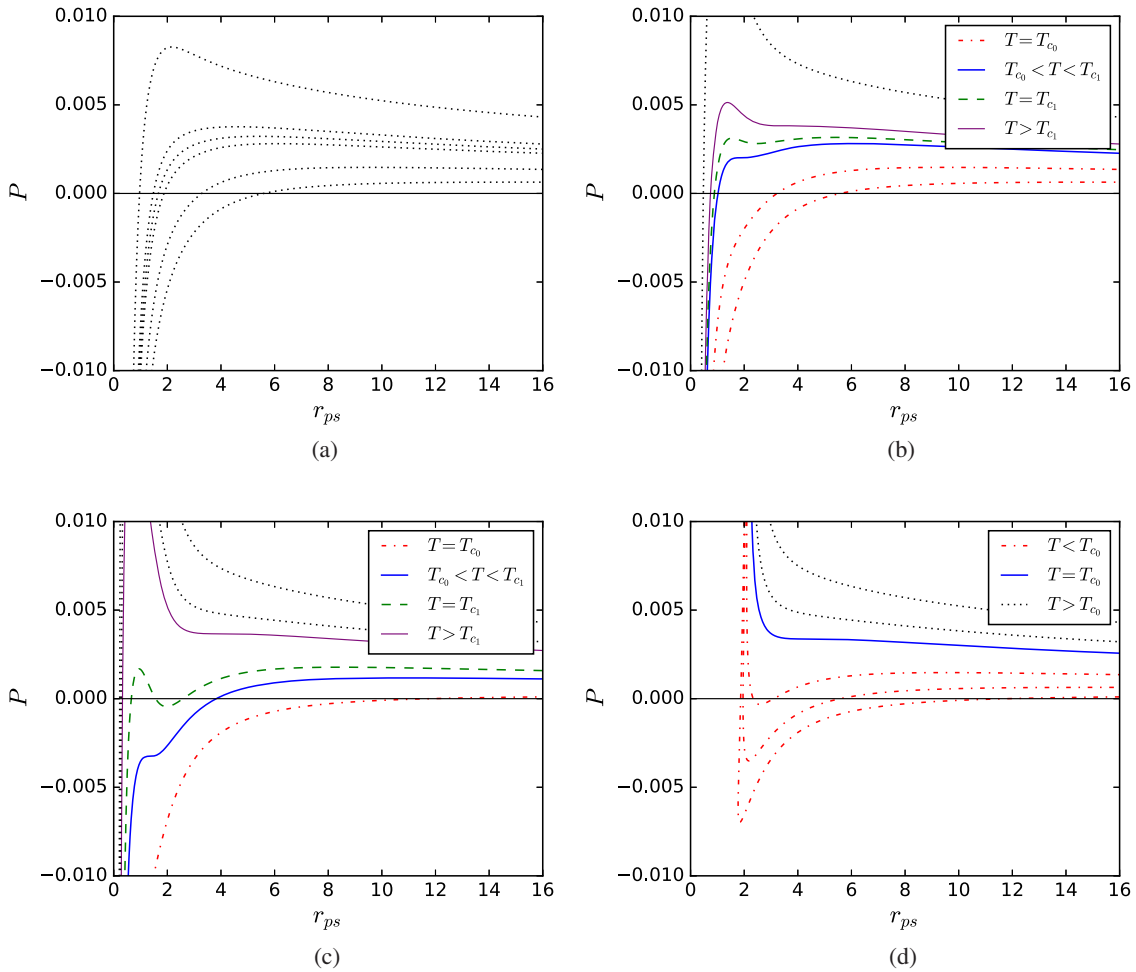

FIG. 10. The pressure P as a function of the radius $r_{\rm ps}$ of the photon sphere for different values of the BI parameter b with fixed temperature T. (a) $b = 0.3 < b_0$ with $T = 0.02$, 0.03, 0.04, 0.043, and 0.06 from bottom to top. (b) $b = 0.4 \in (b_0, b_1)$ with $T = 0.02$, 0.03, 0.040492 ($T_{\rm c0}$), 0.043, 0.045890 ($T_{\rm c1}$), and 0.06 from bottom to top. (c) $b = 0.45 \in (b_1, b_2)$ with $T = 0.01$, 0.026885 ($T_{\rm c0}$), 0.03, 0.045170 ($T_{\rm c1}$), 0.05, and 0.06 from bottom to top. (d) $b = 1 > b_2$ with $T = 0.001$, 0.002, 0.003372 ($P_{\rm c1}$), 0.004, and 0.006 from bottom to top.

figures, we find that the temperature has a complicated behavior with respect to the radius of the photon sphere. For example, when the pressure $P_{\rm c0} < P < P_{\rm c1}$, the temperature has a decrease-increase-decrease-increase behavior, which is quite different from the case of $b = 0.3$, and can be seen as a sign of the reentrant phase transition. In Fig. 9(d) we show the results for $b = 1$. For this case, only one critical point exists and we find a VdW-like phase transition. When the pressure is lower than the critical values, the temperature first increases, then decreases, and finally increases with the radius of the photon sphere, which is a typical behavior that implies the existence of a VdW-like phase transition.

In Fig. 10 we show the pressure P as a function of the radius $r_{\rm ps}$ of the photon sphere at constant temperatures for different values of the parameter b. We find that the behaviors are quite similar for different values of b. The significant difference is that T and P have opposite behavior with respect to $r_{\rm ps}$. For example, when one increases with $r_{\rm ps}$, the other one decreases. However, the number of extremal points is the same.

Next, let us turn to the behavior of the minimum impact parameter $u_{\rm ps}$ of the photon sphere. In Fig. 11 we display the temperature T as a function of $u_{\rm ps}$ for different values of b at constant pressure. When $b = 0.3$, corresponding to case I [see Fig. 11(a)], we find that at small $u_{\rm ps}$ the temperature T decreases rapidly. Then T increases and approaches a high value at a certain finite $u_{\rm ps}$. However, this behavior does not indicate a VdW-like phase transition. For $b = 0.4$ and 0.45 [shown in Figs. 11(b) and 11(c)] the behaviors of T become more complicated. In particular, for fixed pressure $P_{\rm c0} < P < P_{\rm c1}$, with the increase of $u_{\rm ps}$ the temperature T demonstrates a decrease-increase-decrease-increase behavior, which implies that there exists a reentrant phase transition in the corresponding BI-AdS black hole background. However, when $b = 1 > b_2$ [shown in

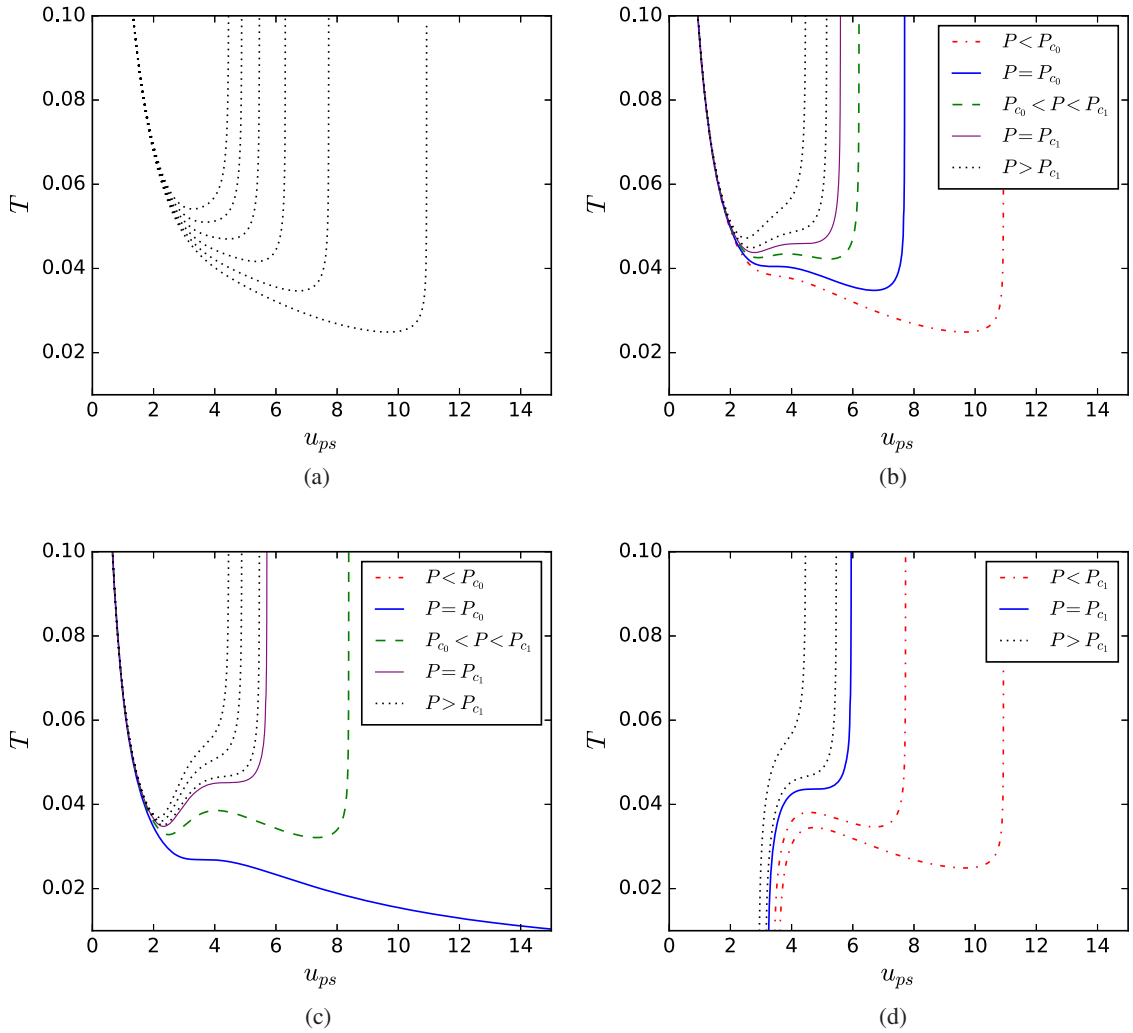

FIG. 11. The temperature T as a function of the minimum impact parameter $u_{\rm ps}$ of the photon sphere for different values of the BI parameter b with fixed pressure P. (a) $b = 0.3 < b_0$ with $P = 0.001$, 0.002, 0.003, 0.004, 0.005, and 0.006 from bottom to top. (b) $b = 0.4 \in (b_0, b_1)$ with $P = 0.001$, 0.002016 ($P_{\rm c0}$), 0.003, 0.003807 ($P_{\rm c1}$), 0.0045 and 0.006 from bottom to top. (c) $b = 0.45 \in (b_1, b_2)$ with $P = -0.003253$ ($P_{\rm c0}$), 0.001,0.002, 0.003, 0.003664 ($P_{\rm c1}$), and 0.006 from bottom to top. (d) $b = 1 > b_2$ with $P = 0.01$, 0.02, 0.03, 0.043620 ($T_{\rm c1}$), 0.05 and 0.06 from bottom to top.

Fig. 11(d)] the black hole system exhibits a VdW-like phase transition. We observe that the temperature shows an increase-decrease-increase behavior for a constant pressure P below its critical value. However, when the pressure is above the critical value, the temperature is only a monotonically increasing function of $u_{\rm ps}$, and thus no phase transition exists for this case.

Moreover, we also plot the pressure P as a function of the minimum impact parameter $u_{\rm ps}$ in Fig. 12. We can see that both the reentrant and VdW-like phase transitions can be identified from the behavior of the pressure P.

In summary, by observing the behavior of the photon sphere of an BI-AdS black hole, both the reentrant phase transition and the VdW-like phase transition can be identified. These two types of phase transitions can be clearly distinguished by the photon sphere. Thus, we confirm our previous conjecture that there indeed exists a relation between the photon sphere and thermodynamic phase transition.

C. Critical behavior of the photon sphere

As discussed above, when $b > b_0$, there will be one or two critical points for BI-AdS black hole systems. However, one of the points has negative pressure or a higher Gibbs free energy, which makes it unstable or unphysical. Nevertheless, one physical critical point always exists for $b > b_0$. Meanwhile, there exists a first-order phase transition between the intermediate and large black holes for $b_0 < b < b_2$, and a first-order phase transition between the small and large black holes for $b > b_2$. With the increase of the pressure and temperature,

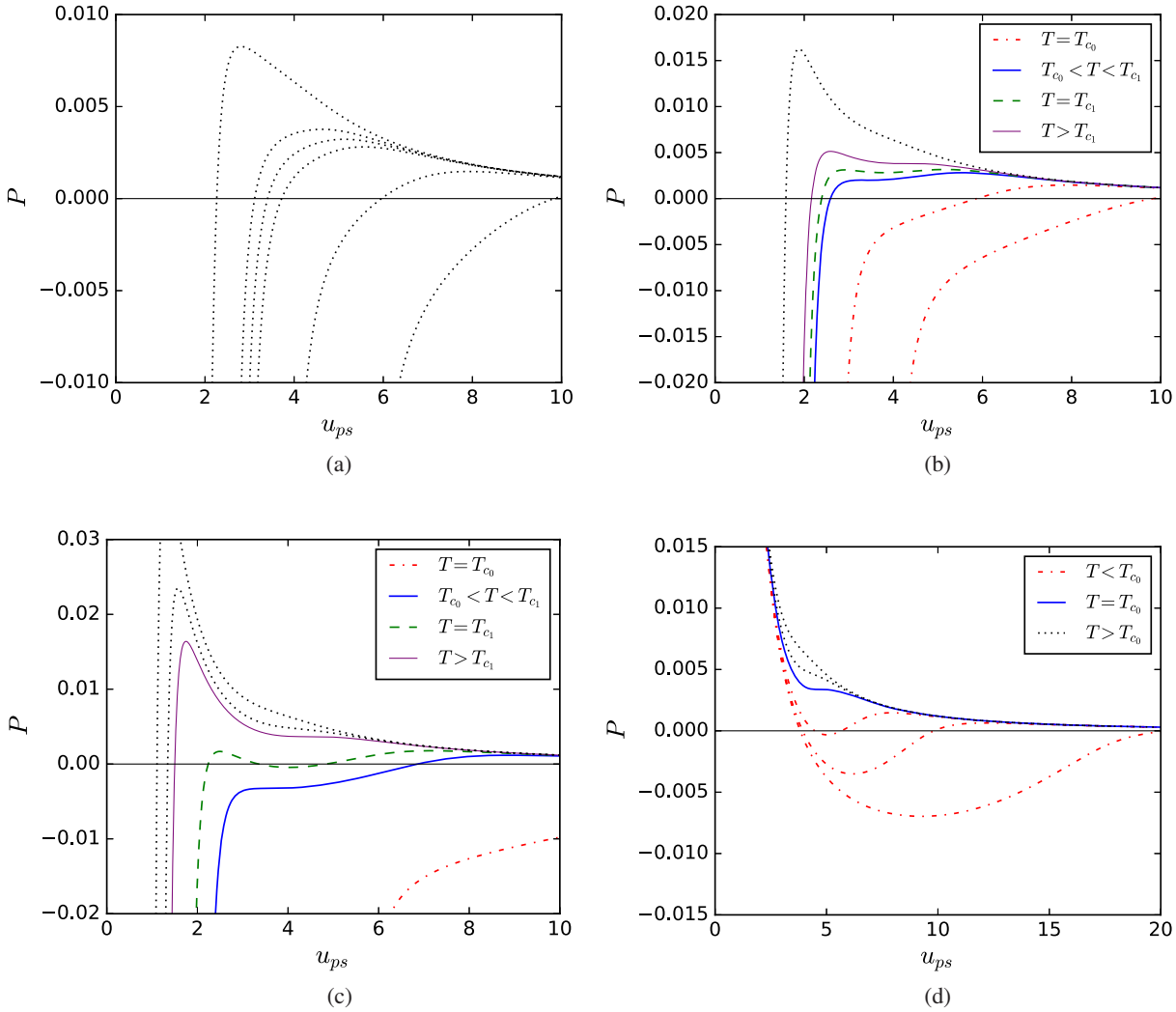

FIG. 12. The pressure P as a function of the minimum impact parameter $u_{\rm ps}$ of the photon sphere for different values of the BI parameter b with fixed temperature T. (a) $b = 0.3 < b_0$ with $T = 0.02$, 0.03, 0.04, 0.043, and 0.06 from bottom to top. (b) $b = 0.4 \in (b_0, b_1)$ with $T = 0.02$, 0.03, 0.040492 ($T_{\rm c0}$), 0.043, 0.045890 ($T_{\rm c1}$) and 0.06 from bottom to top. (c) $b = 0.45 \in (b_1, b_2)$ with $T = 0.01$, 0.026885 ($T_{\rm c0}$), 0.03, 0.045170 ($T_{\rm c1}$), 0.05 and 0.06 from bottom to top. (d) $b = 1 > b_2$ with $T = 0.001$, 0.002, 0.003372 ($P_{\rm c1}$), 0.004 and 0.006 from bottom to top.

these first-order phase transitions terminate at the critical point. Thus, it is worth examining how the radius and minimum impact parameter of the photon sphere change along the coexistence curve and to consider their critical behavior.

Following Refs. [41,42], we $r_{\rm ps}$ and $u_{\rm ps}$ when the first-order phase transition occurs. From Fig. 13, we find that with the increase of the phase transition temperature, both $\Delta r_{\rm ps}$ and $\Delta u_{\rm ps}$ decrease, and when the critical temperature is approached, both of them vanish. This behavior holds for $b > b_0$. Such behaviors are also consistent with that observed in Refs. [41,42].

Next, we calculate the critical exponents of $\Delta r_{\rm ps}$ and $\Delta u_{\rm ps}$ for different values of the BI parameter b. Since there is no analytic result, we use numerical data to fit them as follows [41]:

$$\Delta r_{\rm ps}, \Delta u_{\rm ps} \sim a \times (1 - \tilde{T})^{\delta}, \tag{31}$$

where a and δ are fitting coefficients. If $\Delta r_{\rm ps}$ and $\Delta u_{\rm ps}$ have a universal critical behavior, then the coefficient δ must remain constant for different values of b.

The fitting results are listed in Table I. One can notice that the fitting coefficient a of $\Delta r_{\rm ps}$ and $\Delta u_{\rm ps}$ decreases with b, while the coefficient δ is always around $\frac{1}{2}$ with a numerical error of no more than 1.73% for different values of b. So even when the reentrant phase transition is included, the universal critical exponent does not change.

At last, we examine the consistency between the extremal points of the radius and minimum impact parameter of the photon sphere along the constant temperature or pressure curve and the metastable curve from the thermodynamic side. For a Kerr-AdS black hole, we have shown

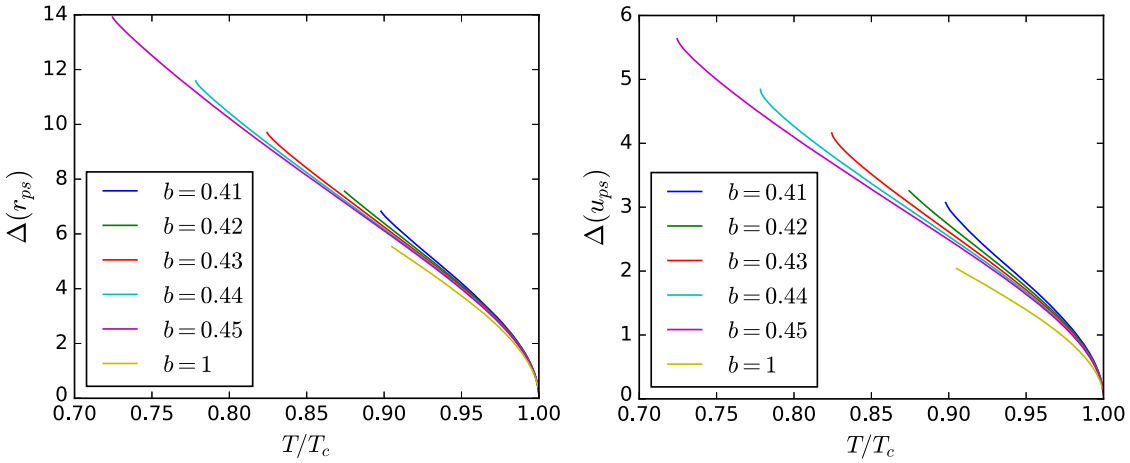

(a) $\Delta r_{\rm ps} - T/T_{\rm c}$ (b) $\Delta u_{\rm ps} - T/T_{\rm c}$

FIG. 13. Behaviors of $\Delta r_{\rm ps}$ and $\Delta u_{\rm ps}$ as a function of the phase transition temperature $T/T_{\rm c}$ for $b = 0.41$–1 from top to bottom.

that they are consistent with each other when the VdW-like phase transition occurs [42]. However, for the case of the reentrant phase transition, the metastable curves became rather interesting; see Figs. 6(a) and 7(a). In Fig. 14 we show the metastable curves (dashed lines) and the extremal point of the radius $r_{\rm ps}$ of the photon sphere (black dots) in the P-T diagram for different values of b. When $b > b_2$ [Fig. 14(d)], the typical VdW phase transition takes place. From this, one can see that these results are highly consistent with each other, which also supports our result for the Kerr-AdS black holes [42]. When $b_0 < b < b_2$, we have the reentrant phase transition; see Figs. 14(b) and 14(c). It is worth noting that there are three metastable curves; however, the extremal points are still in good agreement with the metastable curves. For $b < b_0$, we can also see that they agree with each other even when there is no phase transition. Thus, we confirm that for the entire range of the BI parameter b the extremal points of $r_{\rm ps}$ always coincide with the thermodynamic metastable curves for BI-AdS black holes, and they are independent of the type of phase transition.

IV. NULL GEODESICS AND PHASE TRANSITION FOR HIGHER-DIMENSIONAL BLACK HOLES

In the higher-dimensional BI-AdS black hole cases, i.e., $d \geq 5$, it was found that there is no reentrant phase transition [8], and only the VdW-like phase transition occurs. Here we extend the above treatment of null geodesics to the higher-dimensional cases and examine the behavior of the temperature in terms of $r_{\rm ps}$ and $u_{\rm ps}$.

The metric for d-dimensional BI-AdS black holes is

$$ds^2 = -f(r)dt^2 + \frac{1}{f(r)}dr^2 + r^2 d\Omega_{d-2}^2, \tag{32}$$

where $d\Omega_{(d-2)}^2$ is the line element on the unit $(d-2)$-dimensional sphere $S^{(d-2)}$, and the metric function is given by

$$f(r) = 1 + \frac{r^2}{l^2} - \frac{16\pi M r^{3-d}}{(d-2)\omega_{d-2}} + \frac{4b^2 r^2}{(d-2)(d-1)}\left(1 - \sqrt{\frac{16\pi^2 Q^2 r^{4-2d}}{b^2\omega_{d-2}^2} + 1}\right) \tag{33}$$

$$+ \frac{64\pi^2 Q^2 r^{6-2d}}{(d-3)(d-1)\omega_{d-2}^2} \times {}_2F_1\left(\frac{1}{2}, \frac{d-3}{2d-4}; \frac{3d-7}{2d-4}; -\frac{16\pi^2 Q^2 r^{4-2d}}{b^2\omega_{d-2}^2}\right), \tag{34}$$

TABLE I. Values of the fitting coefficients a and δ near the critical point following the fitting equation (31) for different values of b.

	b	0.41	0.42	0.43	0.44	0.45	1.00
$\Delta r_{\rm ps}$	a	18.059025	17.761526	17.419893	17.173444	17.072752	16.346841
	δ	0.508291	0.507801	0.505974	0.504958	0.505207	0.508663
$\Delta u_{\rm ps}$	a	7.737585	7.508655	7.313941	7.143246	7.041705	6.083478
	δ	0.506776	0.506175	0.505248	0.504228	0.504426	0.506008

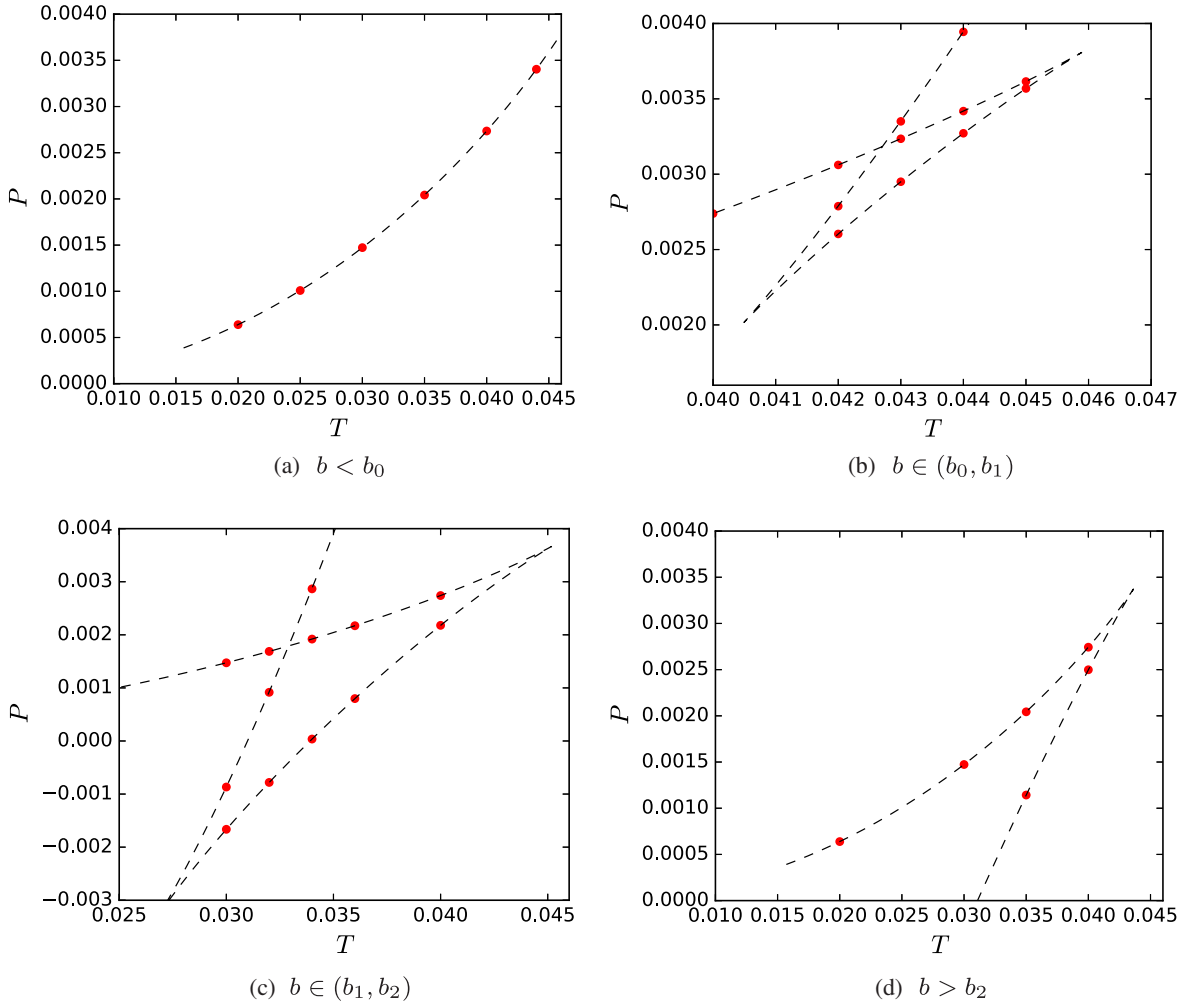

FIG. 14. Extremal points of the radius $r_{\rm ps}$ and the minimal impact parameter $u_{\rm ps}$ of the photon sphere (black dots) and the thermodynamic metastable curves (dashed lines) of BI-AdS black holes shown in the P-T diagram. (a) $b = 0.3$. (b) $b = 0.4$. (c) $b = 0.45$. (d) $b = 1.0$.

where $\omega_{d-2} = \frac{2\pi^{\frac{d-1}{2}}}{\Gamma(\frac{d-1}{2})}$ is the volume of the unit sphere $S^{(d-2)}$. The temperature of the black hole can be calculated as

$$T = \frac{\partial_r f(r_+)}{4\pi} = \frac{(4\pi P + b^2) r_+}{(d-2)\pi} - \frac{b\sqrt{b r_+^{2d}\omega_{d-2}^2 + 16\pi^2 Q^2 r_+^4}}{(d-2)\pi\omega_{d-2} r_+^{d-1}}. \tag{35}$$

Solving for the pressure, we can get the equation of state for black holes,

$$P = \frac{(d-2)T}{4r_+} - \frac{(d-2)(d-3)}{16\pi r_+^2} - \frac{b^2\left(1 - \sqrt{\frac{16\pi^2 Q^2}{b^2\omega^2 r_+^{2d-4}} + 1}\right)}{4\pi}. \tag{36}$$

This equation of state describes a small-large black hole phase transition. The critical point can be obtained by solving

$$(\partial_v P)_T = 0, \qquad (\partial_v^2 P)_T = 0. \tag{37}$$

Since there is no analytical result, we list the critical values of the thermodynamic quantities with fixed $b = 0.1$ and $Q = 1$ for $d = 5$–8 in Table II. From this table we can see that with

TABLE II. Critical values of $v_{\rm c}$, $T_{\rm c}$, $P_{\rm c}$, and $\frac{P_{\rm c} v_{\rm c}}{T_{\rm c}}$ with fixed $b = 0.1$ and $Q = 1$ for $d = 5$, 6, 7, and 8.

d	5	6	7	8
v_c	0.169765	0.309020	0.346222	0.350027
T_c	1.250000	1.030065	1.103263	1.212527
P_c	2.453574	1.249208	1.273844	1.442595
$\frac{P_c v_c}{T_c}$	0.333225	0.374763	0.399754	0.416442

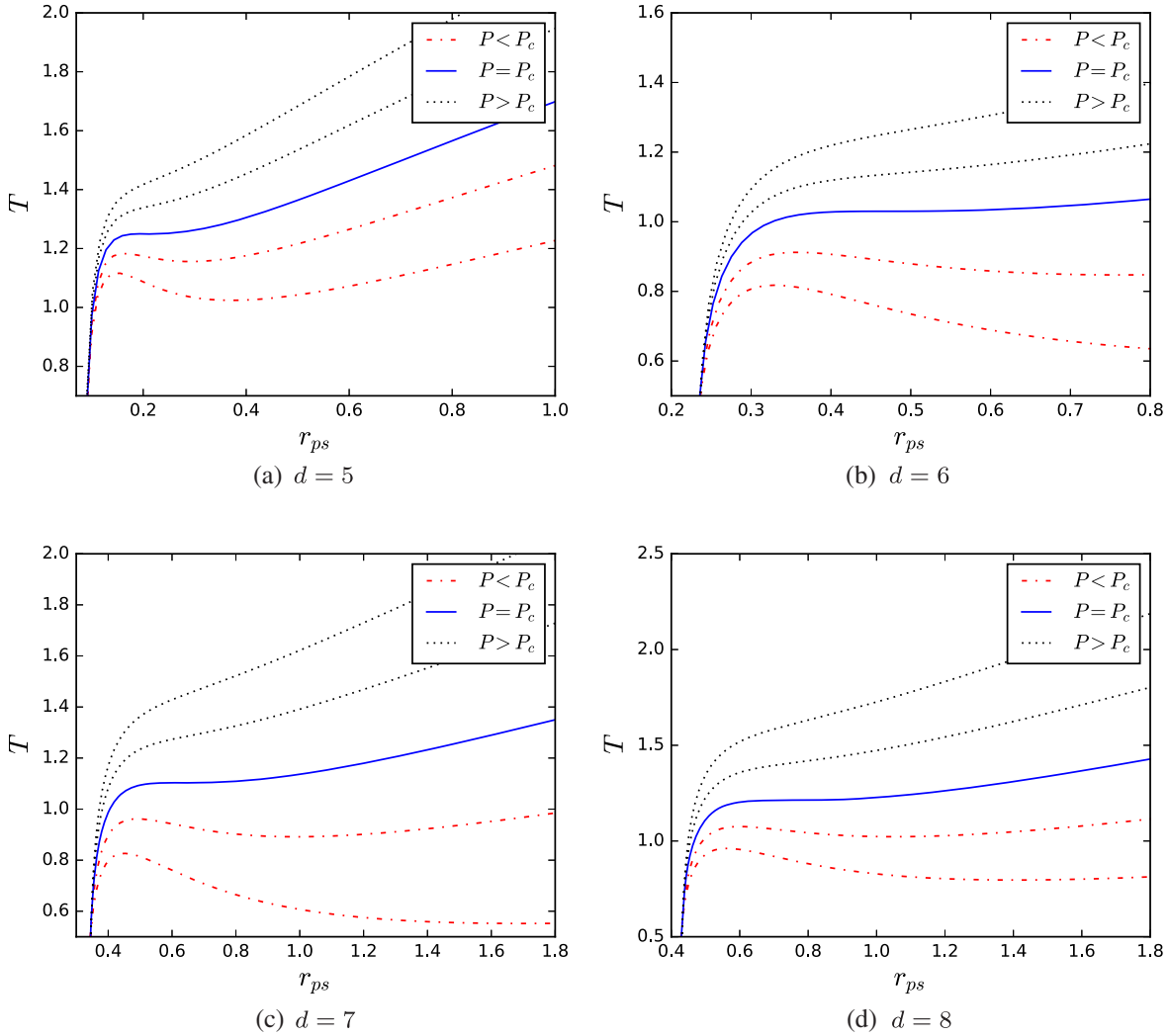

FIG. 15. The temperature T as a function of the radius $r_{\rm ps}$ of the photon sphere with $b=0.1$ and $Q=1$. (a) $d=5$ and the pressure $P=1.5$, 2.0, 2.45357 ($P_{\rm c}$), 3.0, and 3.5 from bottom to top. (b) $d=6$ and the pressure $P=0.4$, 0.8, 1.24921 ($P_{\rm c}$), 1.6, and 2.0 from bottom to top. (c) $d=7$ and the pressure $P=0.3$, 0.8, 1.27384 ($P_{\rm c}$), 1.8, and 2.3 from bottom to top. (d) $d=8$ and the pressure $P=0.6$, 1.0, 1.4426 ($P_{\rm c}$), 2.0, and 2.6 from bottom to top.

the increase of the dimension number d, the value of the critical specific volume $v_{\rm c}$ increases, while the values of $T_{\rm c}$ and $P_{\rm c}$ first decrease, and then increase. Moreover, the dimensionless parameter $\frac{P_{\rm c}v_{\rm c}}{T_{\rm c}}$ is larger than $1/8$ of the four-dimensional charged AdS black hole.

Higher-dimensional black holes also possess a photon sphere, which is also described by Eqs. (28) and (29) as for four-dimensional case. For simplicity, we plot the temperature T as function of $r_{\rm ps}$ and $u_{\rm ps}$ in Figs. 15 and 16, respectively.

In Fig. 15 the temperature T is plotted against $r_{\rm ps}$ for $d=5$, 6, 7, and 8. It is clear that when the pressure $T<T_c$, the temperature first increases, then decreases, and finally increases with $r_{\rm ps}$. This behavior typically indicates a VdW-like phase transition. We can also see that this behavior disappears when $T\geq T_c$, so the small-large black hole can be identified by the radius of the photon sphere. This result is also independent of the dimension d of the spacetime.

In Fig. 16 the temperature T is plotted against the minimum impact parameter $u_{\rm ps}$ for $d=5$, 6, 7, and 8. For a fixed pressure P below the critical value, with the increase of $u_{\rm ps}$ the temperature has an increase-decrease-increase behavior. Above the critical value, this behavior also disappears.

In summary, with the increase of $r_{\rm ps}$ or $u_{\rm ps}$, the behavior of the temperature is similar to that of the four-dimensional black hole case with $b=1$ given in Sec. III. So the

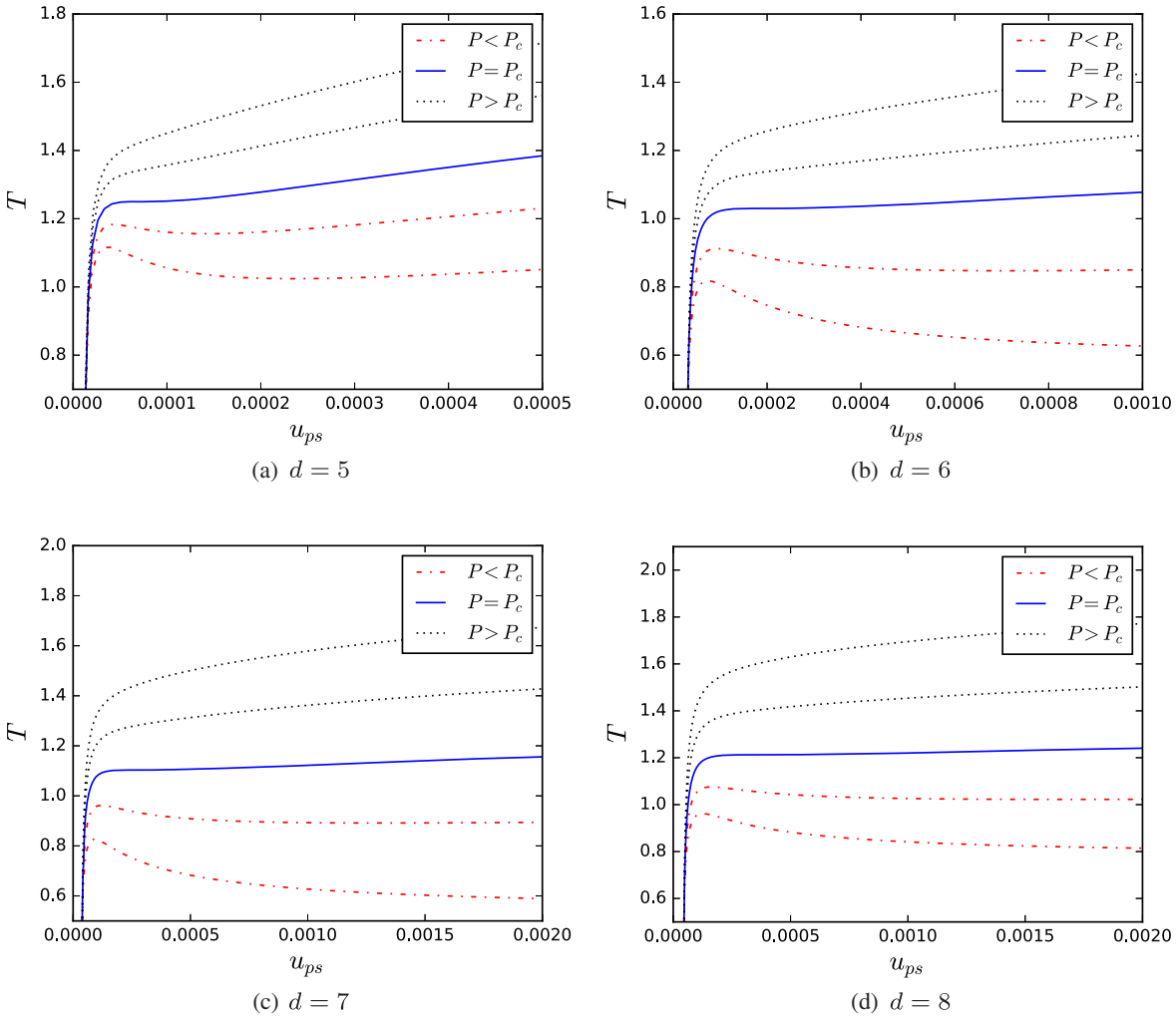

FIG. 16. The temperature T as a function of the minimum impact parameter $u_{\rm ps}$ of the photon sphere with $b = 0.1$ and $Q = 1$. (a) $d = 5$ and the pressure $P = 1.5$, 2.0, 2.45357 ($P_{\rm c}$), 3.0, and 3.5 from bottom to top. (b) $d = 6$ and the pressure $P = 0.4$, 0.8, 1.24921 ($P_{\rm c}$), 1.6, and 2.0 from bottom to top. (c) $d = 7$ and the pressure $P = 0.3$, 0.8, 1.27384 ($P_{\rm c}$), 1.8, and 2.3 from bottom to top. (d) $d = 8$ and the pressure $P = 0.6$, 1.0, 1.4426 ($P_{\rm c}$), 2.0, and 2.6 from bottom to top.

small-large black hole phase transition can occur even in higher-dimensional BI-AdS black holes.

It is worth examining the critical exponents of $\Delta r_{\rm ps}$ and $\Delta u_{\rm ps}$ at the critical point. We first numerically calculate $\Delta r_{\rm ps}$ and $\Delta u_{\rm ps}$, and then fit the data with Eq. (31). The results are listed in Table III. Obviously, the fitting coefficient is always around 0.5 for different d. So one can conclude that $\Delta r_{\rm ps}$ and $\Delta u_{\rm ps}$ have a universal critical exponent of $\frac{1}{2}$. This result confirms that four-dimensional BI-AdS black holes and d-dimensional charged AdS black holes share the same critical exponent [41].

TABLE III. Values of the fitting coefficients a and δ near the critical point following the fitting equation (31) for $d = 5$, 6, 7, and 8 with $b = 0.1$ and $Q = 1$.

	d	5	6	7	8
$\Delta r_{\rm ps}$	a	0.821686	1.465679	1.702252	1.758366
	δ	0.506893	0.497529	0.500749	0.499735
$\Delta u_{\rm ps}$	a	0.000711	0.001931	0.003142	0.004750
	δ	0.548137	0.531734	0.544612	0.514444

V. CONCLUSIONS AND DISCUSSIONS

In this paper we studied the relationship between the null geodesic and thermodynamic reentrant phase transition of BI-AdS black holes by examining the radius $r_{\rm ps}$ and the minimal impact parameter $u_{\rm ps}$ of the photon sphere.

We started with the state equation of BI-AdS black holes. It was shown that the thermodynamic properties are closely dependent on the BI parameter b. According to the number of critical points of the phase transition, the region of b is divided into four cases: $b < b_0$ (case I), $b \in (b_0, b_1)$ (case II), $b \in (b_1, b_2)$ (case III), and $b > b_2$ (case IV). In case I there is no phase transition, while in cases II and III there

are two critical points and a typical reentrant phase transition. The tiny difference between them is that one of the critical points is positive in case II and negative in case III. However, since they have a higher Gibbs free energy, they will not appear in the phase diagram of the black hole system. For case IV there is only one critical point, and thus only a VdW-like phase transition is shown. For the three cases with $b > b_0$, the reentrant and VdW-like phase transitions were described in the P-T phase diagram; see Figs. 6–8. The extremal point curves were also plotted. It is clear that the critical points always occur at the interaction point of the two extremal-point curves. Also, the "zeroth"-order phase transition curve coincides with the extremal-point curves. We also used the T-v phase diagram. For the reentrant phase diagram, the coexistence of the intermediate and large black hole cannot be extended to $T = 0$, while ends at a certain temperature, where the "zeroth"-order phase transitions start.

Next, we followed the Lagrangian of a free photon to obtain the null geodesics for the black holes. Employing the effective potential of radial motion, we numerically solved for the radius r_{ps} and the minimal impact parameter u_{ps} of the photon sphere for BI-AdS black holes. The results also indicate that these quantities are closely dependent on the black hole charge and BI parameter. Then, in order to find the relationship between the photon sphere and the phase transition, we plotted the temperature and pressure in terms of r_{ps} and u_{ps}, respectively, for different values of b.

We obtained the temperature T for fixed pressure P as a function of r_{ps} and u_{ps} (Figs. 9 and 11, respectively). The temperature behaves very differently for the different types of phase transitions, and thus the phase transition can be identified from the behavior of the temperature. In particular, the reentrant phase transition can be identified from the decrease-increase-decrease-increase behavior of the temperature with the increase of r_{ps} and u_{ps}.

We then obtained the pressure P for fixed temperature T as a function of r_{ps} and u_{ps} (Figs. 10 and 12, respectively). P also behaves differently for different values of b. With the increase of r_{ps} or u_{ps}, a reentrant phase transition can take place if the pressure exhibits an increase-decrease-increase-decrease behavior.

We also examined the critical behaviors of r_{ps} and u_{ps} near the critical point. Since only one of the critical points is physical when $b > b_0$, we fitted the formula (31) with the numerical results near the critical point. The results are shown in Table I. The fitting coefficient a for both Δr_{ps} and Δu_{ps} decreases with the parameter b, while it is obvious that the fitting coefficient δ is around $\frac{1}{2}$ with a numerical error of no more than 1.73%. Therefore, Δr_{ps} and Δu_{ps} have a universal critical exponent of $\frac{1}{2}$. These results are exactly consistent with that of the VdW-like phase transition of a charged and rotating AdS black hole given in Refs. [41,42].

Furthermore, we calculated the temperature and pressure corresponding to the extremal points of the radius r_{ps} and minimal impact parameter u_{ps} of the photon sphere. For different values of b, our results show that they completely agree with that of the metastable curves obtained from the thermodynamic side (see Fig. 14). This property also holds even for $b < b_0$, where no reentrant or VdW-like phase transition exists.

Finally, we extended the study to higher-dimensional BI-AdS black holes. The results indicate that the small-large black hole phase transition in higher-dimensional cases can also be identified from the null geodesics. In particular, at the critical point Δr_{ps} and Δu_{ps} also have a universal critical exponent of $\frac{1}{2}$.

In conclusion, we have investigated the relationship between the photon sphere and the thermodynamic phase transition for charged BI-AdS black holes. All of the results imply that information about the reentrant and VdW-like phase transitions of the black holes are encoded in and can be identified by the properties of the photon sphere. The reentrant phase transition can also be distinguished from the VdW-like phase transition through the photon sphere.

ACKNOWLEDGMENTS

This work was supported by the National Natural Science Foundation of China (grants No. 11675064, No. 11875151, and No. 11522541). S.-W. W. was also supported by the Chinese Scholarship Council (CSC) Scholarship (201806185016) to visit the University of Waterloo.

[1] J. D. Bekenstein, Black holes and entropy, Phys. Rev. D **7**, 2333 (1973).
[2] J. M. Bardeen, B. Carter, and S. W. Hawking, The four laws of black hole mechanics, Commun. Math. Phys. **31**, 161 (1973).
[3] D. Kastor, S. Ray, and J. Traschen, Enthalpy and the mechanics of AdS black holes, Classical Quantum Gravity **26**, 195011 (2009).
[4] B. P. Dolan, The cosmological constant and black-hole thermodynamic potentials, Classical Quantum Gravity **28**, 125020 (2011).
[5] M. Cvetic, G. W. Gibbons, D. Kubiznak, and C. N. Pope, Black hole enthalpy and an entropy inequality for the thermodynamic volume, Phys. Rev. D **84**, 024037 (2011).

[6] D. Kubiznak and R. B. Mann, *P-V* criticality of charged AdS black holes, J. High Energy Phys. 07 (2012) 033.
[7] S. Gunasekaran, D. Kubiznak, and R. B. Mann, Extended phase space thermodynamics for charged and rotating black holes and Born-Infeld vacuum polarization, J. High Energy Phys. 11 (2012) 110.
[8] D.-C. Zou, S.-J. Zhang, and B. Wang, Critical behavior of Born-Infeld AdS black holes in the extended phase space thermodynamics, Phys. Rev. D **89**, 044002 (2014).
[9] N. Altamirano, D. Kubiznak, and R. B. Mann, Reentrant phase transitions in rotating AdS black holes, Phys. Rev. D **88**, 101502(R) (2013).
[10] N. Altamirano, D. Kubiznak, R. B. Mann, and Z. Sherkatghanad, Kerr-AdS analogue of triple point and solid/liquid/gas phase transition, Classical Quantum Gravity **31**, 042001 (2014).
[11] A. M. Frassino, D. Kubiznak, R. B. Mann, and F. Simovic, Multiple reentrant phase transitions and triple points in lovelock thermodynamics, J. High Energy Phys. 09 (2014) 080.
[12] S.-W. Wei and Y.-X. Liu, Triple points and phase diagrams in the extended phase space of charged Gauss-Bonnet black holes in AdS space, Phys. Rev. D **90**, 044057 (2014).
[13] B. P. Dolan, A. Kostouki, D. Kubiznak, and R. B. Mann, Isolated critical point from Lovelock gravity, Classical Quantum Gravity **31**, 242001 (2014).
[14] S.-W. Wei, P. Cheng, and Y.-X. Liu, Analytical and exact critical phenomena of *d*-dimensional singly spinning Kerr-AdS black holes, Phys. Rev. D **93**, 084015 (2016).
[15] R. A. Hennigar, R. B. Mann, and E. Tjoa, Superfluid Black Holes, Phys. Rev. Lett. **118**, 021301 (2017).
[16] M. Zhang, D.-C. Zou, and R.-H. Yue, Reentrant phase transitions of topological AdS black holes in four-dimensional Born-Infeld-massive gravity, Adv. High Energy Phys. **2017**, 3819246 (2017).
[17] S. H. Hendi, B. E. Panah, and S. Panahiyan, Einstein-Born-Infeld-massive gravity: AdS-black hole solutions and their thermodynamical properties, J. High Energy Phys. 11 (2015) 157.
[18] S. H. Hendi, B. E. Panah, and S. Panahiyan, Thermodynamical structure of AdS black holes in massive gravity with stringy gauge-gravity corrections, Classical Quantum Gravity **33**, 235007 (2016).
[19] S. H. Hendi, G.-Q. Li, J.-X. Mo, S. Panahiyan, and B. E. Panah, New perspective for black hole thermodynamics in Gauss-Bonnet-Born-Infeld massive gravity, Eur. Phys. J. C **76**, 571 (2016).
[20] S. H. Hendi, R. B. Mann, S. Panahiyan, and B. EslamPanah, Van der Waals like behaviour of topological AdS black holes in massive gravity, Phys. Rev. D **95**, 021501(R) (2017).
[21] D. Momeni, M. Faizal, K. Myrzakulov, and R. Myrzakulov, Fidelity susceptibility as holographic PV-criticality, Phys. Lett. B **765**, 154 (2017).
[22] S. Chakraborty and T. Padmanabhan, Thermodynamical interpretation of the geometrical variables associated with null surfaces, Phys. Rev. D **92**, 104011 (2015).
[23] S.-W. Wei and Y.-X. Liu, Insight into the Microscopic Structure of an AdS Black Hole from Thermodynamic Phase Transition, Phys. Rev. Lett. **115**, 111302 (2015).
[24] J. Jing and Q. Pan, Quasinormal modes and second order thermodynamic phase transition for Reissner-Nordström black hole, Phys. Lett. B **660**, 13 (2008).
[25] E. Berti and V. Cardoso, Quasinormal modes and thermodynamic phase transitions, Phys. Rev. D **77**, 087501 (2008).
[26] X. He, S. Chen, B. Wang, R.-G. Cai, and C.-Y. Lin, Quasinormal modes in the background of charged Kaluza-Klein black hole with squashed horizons, Phys. Lett. B **665**, 392 (2008).
[27] X. He, B. Wang, and S. Chen, Quasinormal modes of charged squashed Kaluza-Klein black holes in the Gödel Universe, Phys. Rev. D **79**, 084005 (2009).
[28] K. Lin, J. Li, and N. Yang, Dynamical behavior and nonminimal derivative coupling scalar field of Reissner-Nordstroem black hole with a global monopole, Gen. Relativ. Gravit. **43**, 1889 (2011).
[29] Q.-Y. Pan and R.-K. Su, Quasinormal modes of phantom scalar perturbation in background of Reissner-Nordstrom black hole, Commun. Theor. Phys. **55**, 221 (2011).
[30] Y. Liu, D.-C. Zou, and B. Wang, Signature of the Van der Waals like small-large charged AdS black hole phase transition in quasinormal modes, J. High Energy Phys. 09 (2014) 179.
[31] D.-C. Zou, Y. Liu, C.-Y. Zhang, and B. Wang, Dynamical probe of thermodynamical properties in three-dimensional hairy AdS black holes, Europhys. Lett. **116**, 40005 (2016).
[32] S. Mahapatra, Thermodynamics, phase transition and quasinormal modes with Weyl corrections, J. High Energy Phys. 04 (2016) 142.
[33] M. Chabab, H. El Moumni, S. Iraoui, and K. Masmar, Behavior of quasinormal modes and high dimension RNAdS black hole phase transition, Eur. Phys. J. C **76**, 676 (2016).
[34] D.-C. Zou, Y. Liu, and R.-H. Yue, Behavior of quasinormal modes and Van der Waals-like phase transition of charged AdS black holes in massive gravity, Eur. Phys. J. C **77**, 365 (2017).
[35] R. Tharanath, N. Varghese, and V. C. Kuriakose, Phase transition, quasinormal modes and Hawking radiation of Schwarzschild black hole in quintessence field, Mod. Phys. Lett. A **29**, 1450057 (2014).
[36] P. Prasia and V. C. Kuriakose, Quasi normal modes and P-V criticallity for scalar perturbations in a class of dRGT massive gravity around Black Holes, Gen. Relativ. Gravit. **48**, 89 (2016).
[37] P. Prasia and V. C. Kuriakose, Quasinormal modes and thermodynamics of linearly charged btz black holes in massive gravity in (Anti) de Sitter space time, Eur. Phys. J. C **77**, 27 (2017).
[38] B. Liang, S.-W. Wei, and Y.-X. Liu, Quasinormal modes and Van der Waals like phase transition of charged AdS black holes in Lorentz symmetry breaking massive gravity, Int. J. Mod. Phys. D **28**, 1950113 (2019).
[39] A.-C. Li, H.-Q. Shi, and D.-F. Zeng, Phase structure and QNMs of a charged AdS dilaton black hole, Phys. Rev. D **97**, 026014 (2018).
[40] M. Zhang and R.-H. Yue, Phase transition and quasinormal modes for spherical black holes in 5D Gauss-Bonnet gravity, Chin. Phys. Lett. **35**, 040401 (2018).

[41] S.-W. Wei and Y.-X. Liu, Photon orbits and thermodynamic phase transition of d-dimensional charged AdS black holes, Phys. Rev. D **97**, 104027 (2018).

[42] S.-W. Wei, Y.-X. Liu, and Y.-Q. Wang, Probing the relationship between the null geodesics and thermodynamic phase transition for rotating Kerr-AdS black holes, Phys. Rev. D **99**, 044013 (2019).

[43] C. Bhamidipati and S. Mohapatra, A note on circular geodesics and phase transitions of black holes, Phys. Lett. B **791**, 367 (2019).

[44] S.-Z. Han, J. Jiang, M. Zhang, and W.-B. Liu, Photon orbits and thermodynamic phase transition in Gauss-Bonnet AdS black holes, arXiv:1812.11862.

[45] M. Chabab, H. El Moumni, S. Iraoui, and K. Masmar, Probing correlation between photon orbits and phase structure of charged AdS black hole in massive gravity background, arXiv:1902.00557.

[46] M. Zhang, S.-Z. Han, J. Jiang, and W.-B. Liu, Circular orbit of a test particle and phase transition of a black hole, Phys. Rev. D **99**, 065016 (2019).

[47] M. Cvetic, G. W. Gibbons, and C. N. Pope, Photon spheres and sonic horizons in black holes from supergravity and other theories, Phys. Rev. D **94**, 106005 (2016).

[48] G. W. Gibbons, C. M. Warnick, and M. C. Werner, Light-bending in Schwarzschild-de-Sitter: Projective geometry of the optical metric, Classical Quantum Gravity **25**, 245009 (2008).

[49] Z.-Y. Tang, Y. C. Ong, and B. Wang, Lux in obscuro II: Photon orbits of extremal AdS black holes revisited, Classical Quantum Gravity **34**, 245006 (2017).